A Practical Channel Modeling Method for Few-mode Optical Fiber Communication Systems

Doohwan Lee†, Kohki Shibahara†, Tadao Nakagawa†, Yutaka Miyamoto†
†NTT Network Innovation Laboratories, NTT Corporation
1-1 Hikarinooka, Yokosuka-shi, Kanagawa, 239-0847 Japan
E-mail: lee.doohwan@lab.ntt.co.jp

Chitradeep Majumdar ‡
‡ Research Center for Advanced Science and Technology, The University of Tokyo
4-6-1 Komaba, Meguro-ku, Tokyo 153-8904 Japan

***Abstract*— A channel modeling method is developed and proposed to practically model the various effects of mode couplings for optical communication systems with multi-core fiber (MCF) and/or few-mode fiber (FMF). The method is similar to existing channel modeling methods in which strong coupling is exclusively considered but extends them to cover both strong and weak couplings. With the method, the entire channel is divided into *K* statistically independent sections where each section may represent an optical device or the span of a few-mode fiber transmission line that maintains coherence. Each section is modeled by a channel matrix model comprising full random unitary matrices and a differential mode delay (DMD) matrix. To further enhance the modeling of weak coupling, the matrix is modified by segregating it into partial block matrices and inserting correlation terms among blocks. The method is evaluated with data obtained in two representative cases: midrange (40 km) and long-haul (527 km) transmissions. Its effectiveness and practicality are validated from agreement obtained between simulation and measured results for the two cases.**

Keywords*— *few-mode fiber; multi-core fiber; channel modeling; mode differential delay; mode coupling; mode division multiplexing

I. Introduction

In recent years, spatial domain multiplexing [1-2] has helped to greatly extend the transmission capacity of optical communication systems. This can be credited to the parallel extension of transmission capacity that has been achieved through the use of mode division multiplexing (MDM). Both optical communication over multi-core fiber (MCF) and/or few-mode fiber (FMF) are included in MDM. To fully utilize the potential transmission capacity increase MDM can provide it is essential to take advantages of the well-developed MIMO signal processing technologies [3]. In particular, it is important to investigate channel models for MCF and/or FMF since the way MIMO signal processing is used might vary depending on the channel model [4]. The effect of couplings among modes is more significant than the effect of couplings among cores in practice. Taking this practical aspect into account, we focused our study on a channel model for FMF.

Optical communication transmission systems have features that differ from those of wireless communication systems, a fact that should be taken into account when developing a channel model. In MIMO wireless communication using multiple antennas, the light speed of each stream is identical and the channel propagation model of each stream is modeled on the basis of an identical statistical model. In contrast, in optical communication over FMF, all modes have different speed, propagation, and attenuation values. These differences are caused by the characteristics of the optical fibers, such as distribution of refractive index inside the fiber. As a result, differential mode delay (DMD) and mode dependent loss (MDL) are uniquely observed in optical communication. To develop an FMF channel model that takes DMD and/or MDL effects into account, particular care should be taken in dealing with mode coupling effects because mode coupling is relevant to the unique features of FMF.

There are two types of mode coupling: strong coupling and weak coupling [4]. These respectively refer to cases in which each mode is statistically fully coupled or partially coupled with other modes. In strong coupling models, the probabilities of mixing or transition of signals between the different polarizations in the same mode and signals between different modes yield identical distributions. Both DMD and MDL can be reduced in the strong coupling case due to the averaging effect that comes from the full interaction among different modes and different polarizations. On the other hand, in weak coupling models, the probabilities of mixing and transition of signals between the same modes and between different modes are not the same. In practice, coupling between the same modes occurs with higher probability than that between different modes in the weak coupling case.

Work done on channel modeling in the strong coupling case has been reported in the literature [3-4]. In this work, the authors assumed that an FMF channel model eventually becomes a strong coupling model. On the basis of this assumption they provided analysis and derivations of DMD and MDL distributions. They justified this assumption by applying the central limit theorem (CLT) assuming the use of a long distance fiber, or by applying the random matrix theory assuming intentionally introduced perturbations in the fiber. Although these models provide a simple and precise mathematical description, there are many cases in practice where the assumption of statistically full coupling does not hold. In addition, without the use of the suggested intentionally perturbed fiber, a system design exclusively based on this strong coupling model may have a practical

‡Currently with Department of Electrical Engineering, Indian Institute of Technology Bombay, India.

limitation because applying the CLT does not guarantee that strong coupling will always be achieved. A recent study considered such a transmission model but it was for direct detection of a 1-km link and irrelevant for our purposes [5].

Therefore it is necessary to consider cases in which both strong and weak couplings simultaneously occur or weak coupling exclusively occurs. This paper extends our previous work [6] and presents a channel modeling method that takes both strong and weak coupling cases into account to provide a more practical channel model. We validated the method's practicality by exploring two representative cases: 1) a midrange distance transmission (40 km) and 2) a long-haul transmission (527 km).

The remainder of this paper is organized as follows. In section II the channel model of the strong coupling mode is presented and extended to include both strong and weak couplings. Section III explains how the model's practicality was validated by exploring two representative case studies. Finally the conclusion and summary of this paper are given in section IV.

II. Channel Model

A. Basic Matrix Channel Propagation Model

We used a matrix channel propagation model that was developed for a strong coupling case [3-4]. Fig. 1 depicts the concept of the model [4]. In the figure, (a) and (b) respectively show the FMF system matrix channel propagation model and its physical representation. The entire channel is divided into K statistically independent sections where each section may represent an optical device or a span of a few-mode fiber transmission line that maintains coherence. The channel propagation matrix of each section represents the channel characteristics of its corresponding physical component.

When the number of modes is equal to D, the channel propagation matrix of the k^{th} $(1 \le k \le K)$ section represented by $\mathbf{M}^k(\omega)$ is given by

$$\mathbf{M}^k(\omega) = \mathbf{V}^k \mathbf{\Lambda}^k(\omega)(\mathbf{U}^k)^*, \tag{1}$$

where * denotes a Hermitian transpose, $\mathbf{V}^k$ and $\mathbf{U}^k$ are $D \times D$ unitary matrices that respectively represent mode coupling at the input and output of the k^{th} section, and $\mathbf{\Lambda}^k(\omega)$ is a diagonal matrix of uncoupled propagation in the k^{th} section. The latter is given as Eq. (2):

$$\Lambda^k(\omega) = \begin{pmatrix} \Lambda_{11}^k(\omega) & 0 & \cdots & 0 \\ 0 & \Lambda_{22}^k(\omega) & \cdots & 0 \\ \vdots & \vdots & \ddots & \vdots \\ 0 & 0 & \cdots & \Lambda_{DD}^k(\omega) \end{pmatrix}, \tag{2}$$

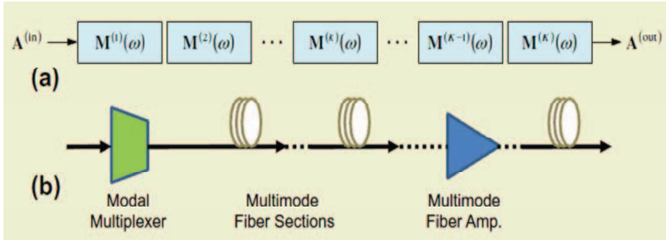

Fig.1 The concept of the channel propagation model [4]. (a) FMF system matrix channel model, (b) Physical representation of the model.

where $\Lambda_{ii}^k(\omega)$ is the i^{th} $(1 \le i \le D)$ diagonal component of $\mathbf{\Lambda}^k(\omega)$ that is equal to $\exp(-j\omega\tau_i)$. Here, τ_i denotes the DMD of the i^{th} mode in the k^{th} section.

Note that the entire channel propagation matrix depends on the frequency dependent characteristics because $\mathbf{\Lambda}^k(\omega)$ consists of the frequency domain representation. On the other hand, both $\mathbf{V}^k$ and $\mathbf{U}^k$ consist of exclusively scalar representations because it is assumed that mode couplings at the input and output of each section do not vary within coherence bandwidth. Hence the usage of this channel model is necessarily limited to within the coherence frequency band.

The entire channel model represented by $\mathbf{M}(\omega)$ is simply obtained by cascading channel propagation matrices of each section as Eq. (3) because the channel propagation matrix of each section is represented in the frequency domain.

$$\mathbf{M}(\omega) = \mathbf{M}^K(\omega)\mathbf{M}^{K-1}(\omega)\cdots\mathbf{M}^2(\omega)\mathbf{M}^1(\omega), \tag{3}$$

B. Extended Matrix Channel Propagation Model

In contrast to the strong coupling model case where $\mathbf{V}^k$ and $\mathbf{U}^k$ are generated by $D \times D$ random unitary matrices, we modify the matrix by segregating it into partial block matrices and inserting correlation terms among blocks when generating $\mathbf{V}^k$ and $\mathbf{U}^k$ [6]. Eq. (4) shows an example of a 6×6 case (three modes with two polarizations).

$$\mathbf{U}_{6\times6}^k, \mathbf{V}_{6\times6}^k = \begin{pmatrix} (1-corr_k)\cdot\mathbf{R}_{2\times2} & corr_k\cdot\mathbf{R}_{2\times4} \\ corr_k\cdot\mathbf{R}_{4\times2} & (1-corr_k)\cdot\mathbf{R}_{4\times4} \end{pmatrix}. \tag{4}$$

In this extended channel propagation model, both strong and weak couplings among different modes are taken into account. The term $corr_k$ $(0 \le corr_k \le 0.5)$ is a tunable parameter representing the correlation between mode LP01 and modes LP11a and LP11b. The 0 and 0.5 values of $corr_k$ respectively represent fully weak and strong couplings. Note that strong couplings between two polarizations and between LP11a and LP11b are assumed in the above example. In Eq. (4), $\mathbf{R}_{2\times2}$, $\mathbf{R}_{2\times4}$, $\mathbf{R}_{4\times2}$, and $\mathbf{R}_{4\times4}$ respectively denote a 2×2 random unitary matrix that represents correlation between two polarizations of mode LP01, a 2×4 matrix generated by two rows of a 4×4 random unitary that represents correlation from LP11a and LP11b to LP01, an 4×2 matrix generated by two columns of a 4×4 random unitary that represents correlation from LP01 to LP11a and LP11b, and a 4×4 random unitary matrix that represents correlation among LP11a and LP11b including their polarizations. In case of a weak coupling between LP11a and LP11b, the matrix representation of $\mathbf{V}^k$ and $\mathbf{U}^k$ is given by a combination of 2×2 partial block matrices.

The channel propagation model of each section is generated by $\mathbf{V}^k \mathbf{\Lambda}^k(\omega)(\mathbf{U}^k)^*$, i.e., the same as Eq. (1). Note that $\mathbf{V}^k$ and $\mathbf{U}^k$ in Eq. (4) are used instead of the $D \times D$ random unitary matrices while the same form of $\mathbf{\Lambda}^k(\omega)$ in Eq. (2) is used to generate the extended channel propagation model of each section. The entire extended channel propagation model is obtained by cascading channel propagation matrices of each section as Eq. (3).

C. Time Domain Channel Model

The time domain channel model that consists of N taps is generated by using N frequency domain channel models to take phase transition due to the time delay into account. Detailed operations are as follows.

First, N different sets of $\mathbf{\Lambda}^k(\omega)$ are generated, of which the i^{th} ($1 \le i \le D$) diagonal element $\Lambda_{ii}^k(\omega)$ is set to $\exp(-j\omega\tau_i t)$, where t spans from 0 to $(N\text{-}1)/N$ with span of $1/N$ ($t = 0, 1/N, \cdots, (N\text{-}1)/N$). This is repeated for all the K sections to generate N different sets of $\mathbf{\Lambda}^k(\omega)$ for each section. Second, $\mathbf{V}^k$ and $\mathbf{U}^k$ of each section are generated by Eq. (4). To generate a time invariant channel, it is not necessary to generate N different sets of $\mathbf{V}^k$ and $\mathbf{U}^k$ because they do not vary within the coherence bandwidth and coherence time. On the other hand, to generate a time varying channel, it is necessary to generate multiple sets of $\mathbf{V}^k$ and $\mathbf{U}^k$. The number of sets is determined on the basis of DMD and coherence time. Third, N different sets of the entire frequency domain channel matrices $\mathbf{M}_l(\omega)$ ($1 \le l \le N$) are generated by Eqs. (1) and (3).

Finally, the IFFT operation of the $N \times 1$ vector, which consists of N elements of the i^{th} row and j^{th} column from all $\mathbf{M}_l(\omega)$, is conducted to find the time domain channel model from mode j to mode i as shown below.

$$\mathrm{h}_{ij}(t) = \mathrm{IFFT}\big(\mathbf{M}_1(i,j), \mathbf{M}_2(i,j), \cdots, \mathbf{M}_N(i,j)\big), \qquad (5)$$

where $\mathrm{h}_{ij}(t)$ and $\mathrm{IFFT}(\cdot)$ respectively denote the time domain channel model from mode j to mode i and the IFFT operation.

All the $D \times D$ elements are obtained by conducting IFFT operations for all elements as depicted in Fig. 2 and

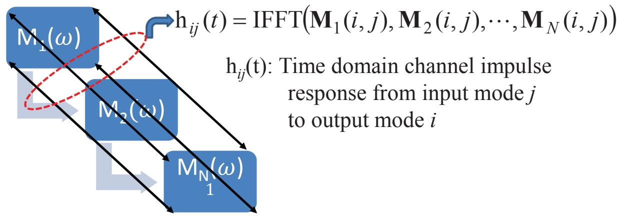

Fig. 2 Generation of the time domain channel model.

correspondingly the time domain channel impulse responses among all modes are obtained.

III. Evaluation

The proposed model was evaluated while varying the number of sections and correlation coefficients. To validate the model's practicality, two representative cases were examined by comparing channel responses of experimental data and those generated from the model. The experimental data were measured for midrange distance transmission (40 km) [1], where strong coupling occurs in the optical devices and weak coupling occurs in the in-between optical fibers, and long-haul transmission (527 km) [2], where the channel model of the midrange transmissions is repeated by loops. In all the evaluation's simulations and experiments we used three modes (LP01, LP11a, and LP11b) with two polarizations. This yielded a 6×6 channel model.

A. Midrange Distance Transmission

The proposed channel model was evaluated using experimental data obtained for a midrange distance transmission (40 km). Some of the representative channel responses are given in Figs. 3 and 4.

Fig. 3 shows a comparison of channel responses between strong and weak coupling. Correlation coefficients were respectively set to be 0.1 and 0.5 for weak and strong coupling models. The number of sections and channel taps was set to 5 for both cases and 1.05-Gbaud signals were used. For the weak coupling model the channel responses between different modes (e.g., *h16*) had a relatively small value while those between the same modes (e.g., *h11*) had a large value. This is because of the rare opportunities for coupling between modes in this case due to low correlation coefficients. On the other hand, for the strong coupling model the channel responses between the same modes and different modes had similar distributions due to the full coupling between modes. These results conform to both intuition and experience and validate the effectiveness of the suggested channel model.

Fig. 4 shows a comparison of channel responses between experimental and simulation data. The DMD and data rate for the experiments were 21 nsec and 0.525-Gbaud with two-fold oversampling [1]. We emulated a channel model to confirm whether the channel modeling data our model generates is sufficiently close to the experimental data. There are two noteworthy points in the experimental data. First, channel responses between the same modes and different modes had similar distribution with two noticeable peaks, which implies nearly full coupling between modes had occurred two times.

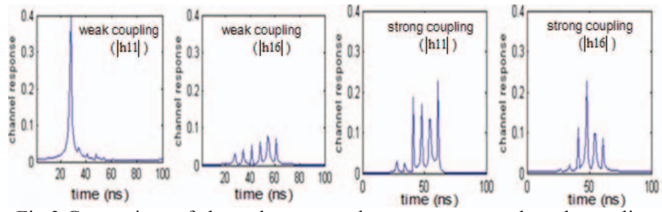

Fig.3 Comparison of channel responses between strong and weak coupling for a midrange distance transmission (40 km).

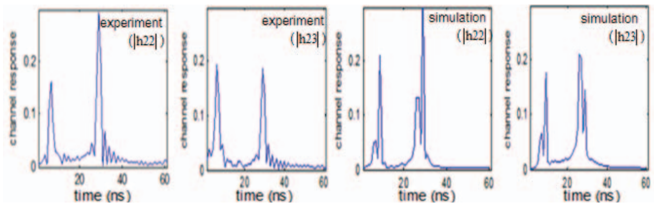

Fig.4 Comparison of channel responses between experiment and simulation for a midrange distance transmission (40 km).

Second, despite the possibility that full coupling had occurred, distributions of channel responses were different from those of strong coupling (Fig. 3), which means that full coupling did not always occur between sections. Accordingly, we adjusted the correlation coefficients between the first and last two consecutive sections to be 0.3 and those between other sections to be 0.001. The number of sections and channel taps were set to be 10 and 60, 1.05-Gbaud signals were used, and DMD per section was set to be 2.5 ns. Simulation results obtained with our channel model were in good agreement with those obtained in the experiments, in which the model's configuration comprised transmitting and receiving optical devices that may cause large coupling and in-between optical fibers that may cause small coupling.

B. Long-haul Transmission

The proposed channel model was also evaluated using experimental data obtained for a long-haul distance transmission (527 km) [2]. Fig. 5 shows the experimental setup of the multi-core few-mode fiber (MC-FMF) transmission. The transmission line was an MC-FMF with 52.7 km length and the long-haul transmission was conducted by repeating the transmission loops over the transmission line. Since this sort of experimental setup is common for both academic and practical purposes it is important to study the channel model for this case.

Even in a single transmission various DMDs were observed due to the large number of parallel transmissions over multi-cores and over different modes. The maximum and average DMD were respectively 33.2 and 15.3 ns for 527 km transmission [2]. The transmission line comprised 12 cores, each of which carried 20 different 12.5 GHz spaced channels (1556.0 - 1557.9 nm). We examined two cases that respectively featured the largest (core #6) and nearest-average DMD (core #10) among all cores for which DMDs were 33.2 and 12 ns. The evaluated wavelength channel was set to 11. The data rate for the experiments was 1-Gbaud with two-fold oversampling. To emulate this experimental setup the number of sections in a single loop and the number of loops were respectively set to be 20 and 10. Correspondingly, the total

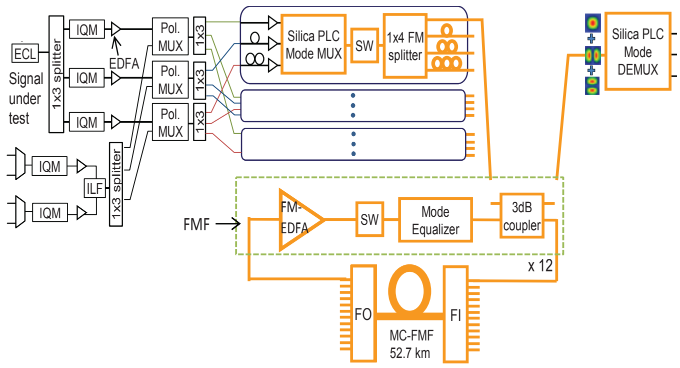

Fig.5 Experimental setup of the long-haul transmission (527 km) with repeated transmission loops [2].

number of sections was equal to 200 to model the 527 km transmission. The number of channel taps was set to be 128, which was around twice the maximum DMD. The correlation coefficients and DMD per section were adjusted to yield both maximum and nearest average DMDs.

There were in all 36 channel responses in each channel because the experiment was also conducted using six different modes. Among them *h42* was examined as a representative channel response. Note that other channel responses also showed similar patterns. Comparisons of channel responses for maximum and average DMD cases between experiments and simulations are given in Fig. 6. We also emulated the channel model to confirm whether the channel modeling data our model generates are sufficiently close to the experimental data. In the case of generating the channel model of the maximum DMD, the correlation coefficients of the first and last three sections were set to be 0.15 to emulate relatively large couplings caused by optical devices such as fan-in/ fan-out device. The correlation coefficients of other sections were set to be 0.001 to emulate weak coupling caused by in-between optical fibers. The DMD of each section were set to be 0.166 ns to match the corresponding experimental results. Similarly, in the case of generating the channel model of the nearest-average DMD, the correlation coefficients of the first and last three sections, the correlation coefficients of other sections, and the DMD of each section were respectively set to be 0.35, 0.0015, and 0.06 ns to match the corresponding experimental results. Note that the DMDs after the concatenation of all 200 sections were set to be equal to those of experiments.

The Fig. 6 results confirmed that the channel responses generated by simulation using the aforementioned parameters are in good agreement with those of the experiments. This shows the effectiveness of the proposed channel modeling method in modeling a long-haul transmission channel. The results also confirm that it is possible to model FMF channels with various DMDs by using the proposed method with proper adjustment of correlation coefficients and DMD per section.

IV. Conclusion

A channel modeling method that can model both strong and weak couplings is suggested by extending the matrix channel propagation model. This method is beneficial for analysis, simulation study, and system design for few-mode fiber optical communication systems. The method's effectiveness and practicality were shown by comparing simulation and measured results for two representative cases, i.e., midrange (40 km) and long-haul (527 km) transmission. In the midrange transmission case, the method successfully emulated experimental data showing that transmitting and receiving devices may cause large coupling and in-between optical fibers may cause weak coupling. In the long-haul transmission case, where the transmission was repeated by midrange transmission loops, the method also successfully emulated the experimental data that showed various DMDs.

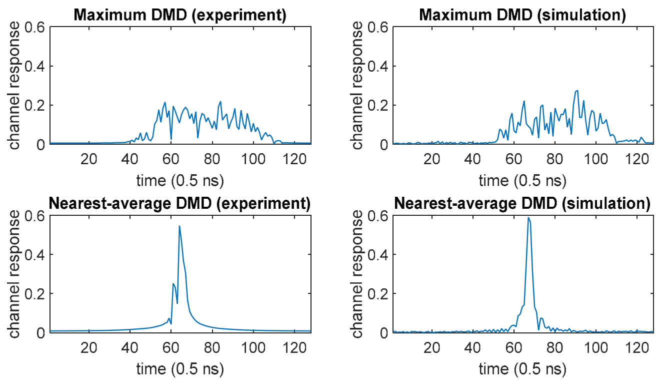

Fig.6 Comparisons of channel responses of |h42| between experiment and simulation for the maximum (core #6) and nearest-average DMD (core #10) cases in a long-haul distance transmission (527 km,).

ACKNOWLEDGMENT

Part of this research used results obtained from research commissioned by the National Institute of Information and Communications Technology (NICT) of Japan. The authors also thank Dr. T. Kobayashi for valuable insight and comments.

REFERENCES

[1] T. Mizuno, T. Kobayashi, H. Takara, A. Sano, H. Kawakami, T. Nakagawa, Y. Miyamoto, Y. Abe, T. Goh, M. Oguma, T. Sakamoto, Y. Sasaki, I. Ishida, K. Takenaga, S. Matsuo, K. Saitoh, and T. Morioka, "12-core x 3-mode Dense Space Division Multiplexed Transmission over 40 km Employing Multi-carrier Signals with Parallel MIMO Equalization," in Proc. Optical Fiber Communication Conference (OFC2014), OFCPD-2014-TH5B.2, pp.1-3, Mar. 2014.

[2] K. Shibahara, T. Mizuno, H. Takara, A. Sano, H. Kawakami, D. Lee, Y. Miyamoto, H. Ono, M. Oguma, Y. Abe, T. Kobayashi, T. Matsui , R. Fukumoto, Y. Amma, T. Hosokawa, S. Matsuo, K. Saito, H. Nasu, and T. Morioka, "Dense SDM (12-core x 3-mode) Transmission over 527 km with 33.2-ns Mode-Dispersion Employing Low-Complexity Parallel MIMO Frequency-Domain Equalization," in Proc. Optical Fiber Communication Conference (OFC2015), OFCPD-2015-TH5C.3, pp.1-3, Mar. 2015.

[3] S. Aric, J. Kahn, and K. Ho, "MIMO Signal Processing for Mode-Division Multiplexing: An overview of channel models and signal processing architectures," IEEE Signal Process. Mag., vol.31, no. 2, pp. 25-34, Mar. 2014.

[4] K. Ho and J. M. Kahn, "Mode Coupling and its Impact on Spatially Multiplexed Systems," Opt. Fiber Telecom. (6th Edition), pp. 491-568 Elsevier, May, 2013.

[5] I. Gasulla and J. Kahn, "Performance of Direct-Detection Mode-Group-Division Multiplexing Using Fused Fiber Couplers," J. Lightw. Technol., vol. 33, no. 9, pp. 1748-1760, May, 2015.

[6] D. Lee, C. Majumdar, T. Nakagawa, T. Kobayashi, and Y. Miyamoto, "A Study on Channel Modeling of Weak Coupling in Multimode Optical," in Proc. IEICE General Conference, B-10-55, Mar. 2015.